

This is a repository copy of *Supraorbital morphology and social dynamics in human evolution.*

White Rose Research Online URL for this paper:

<https://eprints.whiterose.ac.uk/129463/>

Version: Accepted Version

Article:

Godinho, Ricardo Miguel, Spikins, Penny orcid.org/0000-0002-9174-5168 and O'Higgins, Paul orcid.org/0000-0002-9797-0809 (2018) Supraorbital morphology and social dynamics in human evolution. *Nature Ecology and Evolution*. pp. 956-961. ISSN 2397-334X

<https://doi.org/10.1038/s41559-018-0528-0>

Reuse

Items deposited in White Rose Research Online are protected by copyright, with all rights reserved unless indicated otherwise. They may be downloaded and/or printed for private study, or other acts as permitted by national copyright laws. The publisher or other rights holders may allow further reproduction and re-use of the full text version. This is indicated by the licence information on the White Rose Research Online record for the item.

Takedown

If you consider content in White Rose Research Online to be in breach of UK law, please notify us by emailing eprints@whiterose.ac.uk including the URL of the record and the reason for the withdrawal request.

Supraorbital morphology and social dynamics in human evolution

Ricardo Miguel Godinho, Penny Spikins, Paul O'Higgins

Supplementary information

Supplementary Table 1.....	3
Supplementary Table 2.....	4
Supplementary Table 3.....	5
Supplementary Table 4.....	6
Supplementary Figure 1	7
Supplementary Figure 2	8
Supplementary Figure 3.....	10

Supplementary Table 1: applied Muscle Forces (in Newtons).

	Left	Right
Temporalis	168.02	170.67
Masseter	134.06	124.01
Medial pterygoid	124.01	117.49

Supplementary Table 2: landmarks used in the analysis of global deformation.

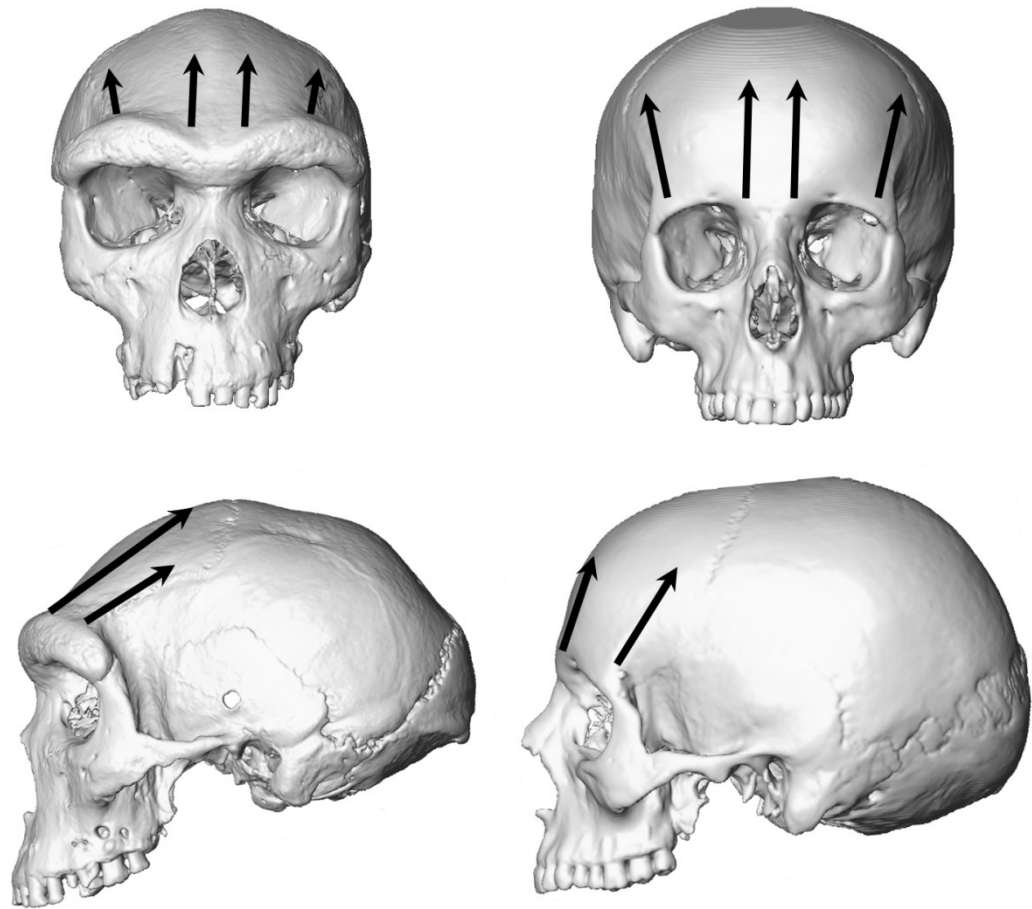
No.	Name	Definition
1	Vertex	Highest point on the midsagittal contour of the calvarium (lateral view in Frankfurt Horizontal).
2	Nasion	Intersection of the frontonasal and internasal suture.
3	Anterior Nasal Spine	Tip of the anterior nasal spine.
4	Prosthion	Most buccal and occlusal point of the interalveolar septum between central incisors.
5	Opistocranum	Most posterior point of the neurocranium.
6; 7	Supraorbital torus	Most anterior point of the supraorbital ridge.
8; 9	Infraorbitale	Most inferior point of the infraorbital ridge.
10; 11	Nasal notch	Most lateral part of the nasal aperture.
12; 13	Ext. Alv. P4	Most buccal and occlusal point on the distal maxillary alveolus of P4
14; 15	Last molar	Last point of the dental arch, located at the most buccal and distal point of the last present molar and alveolar process.
16; 17	Zygo-temporal inferior	Most inferior point of the zygomatico-temporal suture.
18; 19	Fronto-zygomatic	Most lateral point of the fronto-zygomatic suture.
20; 21	Jugale	Deepest point in the notch between the temporal and frontal processes of the zygomatic bone (in Frankfurt Horizontal).
22; 23	Zygomatic Arch lateral	Most lateral point of the zygomatic arch.
24; 25	Zygomatic Root posterior	Most postero-superior point on the intersection between the zygomatic root and the squama of the temporal bone.
26; 27	Zygomatic Root anterior	Most anterior point on the intersection between the zygomatic root and the squama of the temporal bone.
28; 29	Zygomatic Arch medial	Most lateral point of the inner face of the zygomatic arch (superior view in Frankfurt Horizontal).
30; 31	Infratemporal Crest	Tip of the infratemporal crest.
32; 33	Euryon	Most lateral point of the neurocranium in frontal view.

Supplementary Table 3: examples of uniquely human affiliative expressions based on highly mobile eyebrows.

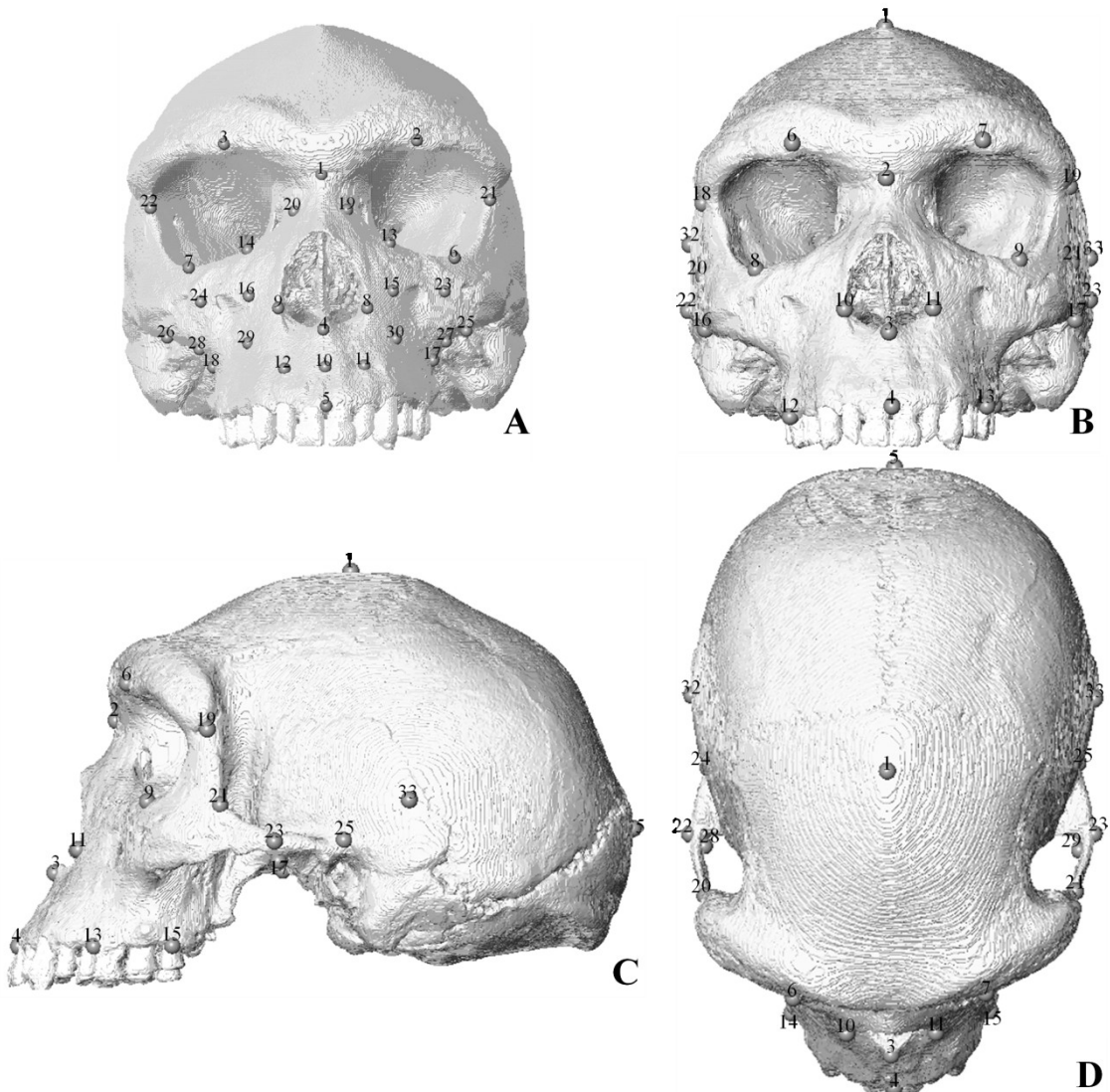
Expression	Description	Reference
Greeting/recognition/contact readiness	'Eyebrow flash' (1/6 th second raise of eyebrows)	Grammer et al. ⁵⁷
Surprise/social indignation	Slow eyebrow raise	Eibl-Eibesfeldt ⁵⁸
Skepticism	Raised outer corner of one eyebrow	Ekman ³
Sympathy	Eyebrows pulled up in the middle	Bavelas et al. ⁵⁹
Trustworthiness/pro-social intention	Dynamic movements of the eyebrows	Hehman et al. ⁶¹

Supplementary Table 4: maximum (ε_1) and minimum (ε_3) principal strains experienced by the models using the original and re-oriented muscle vector directions. Anteroposterior reorientation has a maximum impact of ~5% on average strains. Mediolateral reorientation impacts less than 2%. See anatomical location of landmarks in extended data table 2.

Landmark	ORIENTATION OF MUSCLE VECTORS									
	Original		5° rotation posteriorly		5° rotation anteriorly		5° rotation laterally		5° rotation medially	
	ε_1	ε_3	ε_1	ε_3	ε_1	ε_3	ε_1	ε_3	ε_1	ε_3
1	0.43	-0.86	0.53	-0.80	0.33	-0.99	0.29	-0.54	0.57	-1.20
2	10.26	-15.94	7.86	-10.76	12.59	-21.03	10.35	-16.36	10.13	-15.45
3	19.99	-8.55	17.46	-7.48	22.34	-9.55	20.04	-8.57	19.92	-8.52
4	99.27	-170.50	88.99	-152.73	108.76	-186.95	99.59	-170.60	98.75	-170.04
5	0.11	-0.06	0.14	-0.07	0.14	-0.06	0.13	-0.06	0.17	-0.09
6	3.35	-5.73	2.60	-5.17	4.11	-6.28	3.39	-5.81	3.29	-5.62
7	3.33	-3.13	2.85	-2.94	3.79	-3.30	3.37	-3.21	3.27	-3.04
8	31.20	-37.02	30.46	-35.72	31.76	-38.11	31.91	-38.92	30.42	-35.09
9	24.15	-66.27	22.24	-60.87	25.87	-71.14	24.39	-66.83	23.94	-65.72
10	53.26	-143.42	46.81	-126.02	59.30	-159.71	53.01	-142.74	53.38	-143.77
11	49.30	-140.12	43.41	-122.91	54.82	-156.26	49.08	-139.23	49.39	-140.67
12	9.78	-6.26	8.59	-5.65	10.89	-6.83	10.25	-6.44	9.31	-6.07
13	3.15	-6.12	2.67	-5.39	3.61	-6.81	3.44	-6.29	2.89	-5.93
14	7.59	-10.26	7.11	-9.74	8.02	-10.76	7.70	-9.78	7.45	-10.67
15	3.21	-7.53	3.09	-7.32	3.33	-7.74	3.19	-7.34	3.21	-7.67
16	19.15	-47.47	19.57	-49.64	18.66	-45.02	19.60	-48.61	18.62	-46.19
17	18.26	-38.55	20.06	-46.19	17.16	-31.35	18.37	-36.95	18.15	-40.18
18	20.75	-9.55	19.23	-8.42	22.19	-10.66	20.71	-9.49	20.67	-9.56
19	10.76	-16.72	9.56	-14.69	11.90	-18.61	10.59	-16.20	10.92	-17.23
20	138.57	-52.25	121.88	-45.96	154.20	-58.15	132.18	-49.89	144.04	-54.27
21	142.47	-56.13	127.48	-50.34	156.40	-61.50	138.45	-54.55	145.58	-57.35
22	63.74	-147.25	67.27	-161.85	60.39	-132.06	65.41	-147.49	61.92	-146.77
23	49.27	-96.13	49.76	-107.74	49.79	-84.93	50.89	-94.14	47.61	-98.11
24	24.00	-51.08	22.48	-49.90	25.40	-52.13	23.79	-51.05	24.06	-50.81
25	23.81	-40.88	22.72	-39.67	24.77	-42.05	23.87	-41.24	23.62	-40.30
26	29.61	-22.47	30.67	-21.76	28.59	-23.16	29.04	-22.46	30.18	-22.37
27	110.70	-38.71	116.73	-40.46	104.63	-37.27	108.23	-37.94	112.76	-39.31
28	80.53	-229.40	84.41	-234.10	76.93	-224.29	86.92	-248.91	73.85	-208.80
29	78.56	-225.62	82.03	-235.64	74.64	-214.21	80.51	-230.29	76.32	-220.06
30	5.18	-13.53	4.52	-11.84	6.88	-15.81	5.42	-13.94	4.90	-13.02
31	10.11	-5.04	7.92	-5.46	12.71	-4.95	11.88	-5.10	8.41	-5.07
32	9.10	-9.02	9.45	-9.27	8.68	-8.70	8.65	-9.09	9.50	-8.89
33	9.15	-9.52	9.45	-9.88	8.79	-9.14	8.69	-9.67	9.56	-9.33
Max	142.47	-0.06	127.48	-0.07	156.40	-0.06	138.45	-0.06	145.58	-0.09
Min	0.11	-229.40	0.14	-235.64	0.14	-224.29	0.13	-248.91	0.17	-220.06
Mean	37.28	-56.02	35.36	-55.20	39.11	-56.68	37.20	-57.11	37.21	-55.07
Difference in mean (%)			94.86	98.55	104.93	101.19	99.79	101.95	99.83	98.31



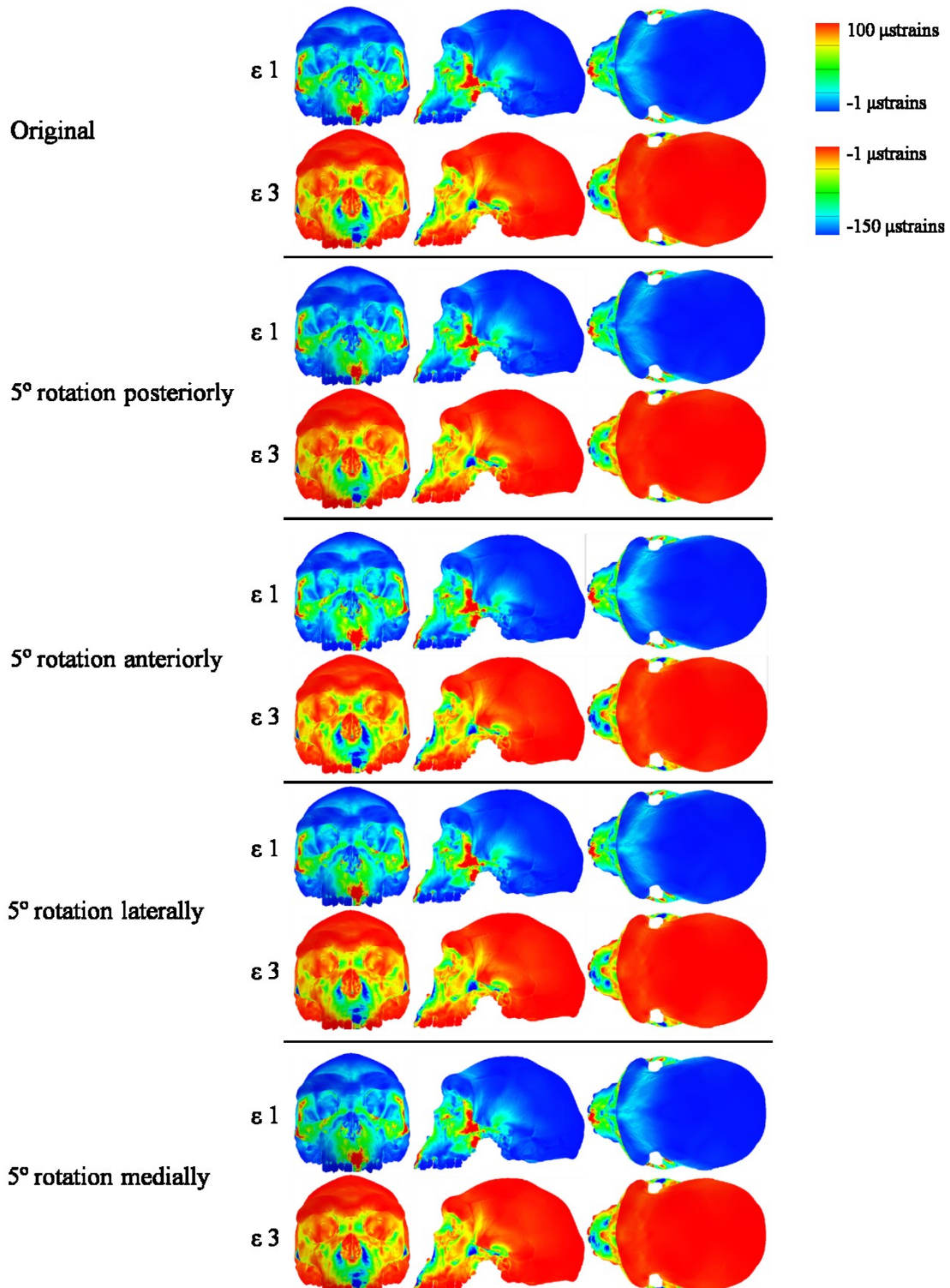
Supplementary Figure 1: Comparison of frontalis muscle vectors orientations. Note the more horizontal orientation of the vectors in Kabwe 1 and the more vertical orientation in the modern human.



Supplementary Figure 2: depiction of the (A) 30 points placed on the facial skeleton to extract ε_1 and ε_3 and of the (B, C, D) 33 cranial landmarks used for the global analysis of deformation (see extended data table 2 for landmark identification and description).

Orientation of muscle vectors

Strain contour plots



Supplementary Figure 3: Maximum (ϵ_1) and minimum (ϵ_3) principal strain contour plots of the sensitivity analysis of errors in muscle vector orientations. The results compare the original estimated directions using the Tabun 1 mandible with different orientations in which the vectors were redirected 5° posteriorly, 5° anteriorly, 5° laterally and 5° medially. Re-orientation of the vectors has a relatively small impact in strains. Extended data table 4 presents the strain magnitudes.